Improved Prediction of Reaction Kinetics for Amine Absorbent-based Carbon Capture using Reactive Site-based Transition State Conformer Search Method

Qilei Liu[a], Sheng Xiang[a], Jian Du[a], Qingwei Meng[a,b], Lei Zhang[a*]

[a]State Key Laboratory of Fine Chemical, Frontiers Science Center for Smart Materials Oriented Chemical Engineering, Institute of Chemical Process Systems Engineering, School of Chemical Engineering, Dalian University of Technology, Dalian 116024, China

[b]Ningbo Research Institute, Dalian University of Technology, Ningbo, 315016, China

Abstract

There is no doubt that carbon emissions are one of the greatest challenges facing humanity today. Carbon capture, utilization, and storage is an effective way to achieve carbon neutrality. However, the commonly used commercial absorbents for post-combustion captures still have some limitations such as low chemical absorption rate constants. In this paper, a universal reaction kinetic model is developed for amine-based carbon capture based on the transition state theory, density functional theory, and hybrid solvation model. The developed reaction kinetic model is applicable to a wide range of amine-solvent solutions involving primary/secondary/tertiary amines and aqueous/nonaqueous solvents. The key contribution of this work is developing a reactive site-based transition state conformer search method, which has greatly improved the prediction accuracy of the reaction kinetic model from R^2=0.819 to R^2=0.943 based on a dataset of 21 various amine-solvent solutions. The results highlight the critical impacts of the transition state conformational isomers on amine-based CO_2

chemical absorption rate constants.

Keywords: Carbon capture; amine absorbent; reaction kinetics; transition state; conformational isomer.

1 Introduction

The increasing development of human society, economy and industry has resulted in a growing demand for fossil fuels in various production activities. As a result of burning fossil fuels, a significant amount of greenhouse gases are produced, causing a series of environmental problems, including global warming and extreme weather conditions. According to the sixth assessment report of the Intergovernmental Panel on Climate Change (IPCC), the average annual global greenhouse gas emissions from 2010 to 2019 were at the highest level in human history, but the growth rate has slowed down. However, the goal of limiting global warming to around 2°C still requires a peak in global greenhouse gas emissions by 2025 at the latest, as well as a quarter decrease in emissions by 2030[1]. As the main gas causing the greenhouse effect, the absorption and disposal of carbon dioxide (CO_2) has always been an issue of widespread concern. Carbon Capture, Utilization and Storage (CCUS) is widely deemed as a key technology to reduce CO_2 emissions from large industrial facilities. According to the IPCC report, modern conventional power plants equipped with CCUS technology can reduce CO_2 emissions to the atmosphere by 80-90%[2]. There is no doubt that CCUS has the potential to reduce CO_2 emissions in the short term, but the high cost and energy requirements of current CO_2 capture methods make it a challenging technological option. Generally, the carbon capture technology can be divided into the pre-combustion capture, oxy-fuel combustion capture, and post-combustion capture[3]. In general, the post-combustion capture is considered the most feasible method of capturing CO_2 as it has a mature technology and is easy to integrate with other industrial

processes. There are a number of common methods for post-combustion capture, including the membrane separation[4, 5], physical adsorption[6, 7], and chemical absorption[8, 9]. Although the membrane separation method is currently considered to be the most potential method for CO_2 capture, it is not widely used in industry due to its late development. The limitation of physical adsorptions is that the amount of absorption is usually not large enough. Chemical absorption first appeared in the 1930s and is widely used in industrial CO_2 capture owe to its advantages of large absorption capacity and fast absorption rate. One of the most important factors in chemical absorptions is the choice of CO_2 absorption medium[10].

There are a number of commonly used absorbents, including the aqueous ammonia[11], potassium carbonate[12], ionic liquid[13], organic amine[14], and so on. Aqueous ammonia absorbents have large absorption capacities and low energy consumptions for regeneration, but their reaction rate is slow and they are highly volatile, making them prone to cause secondary pollution[15]. Potassium carbonates are low in cost and highly stable, but their absorption rates are slow and often require the addition of expensive catalysts[16]. Ionic liquids have low vapor pressure and sound thermal stability, however, they have several disadvantages, including the complicated and costly synthesis steps, high viscosity and a large mass transfer resistance that reduces the heat transfer coefficient[17]. Compared with other absorbents, organic amines have the advantages of large absorption capacity, rapid absorption rate, and low operating costs. Organic amine compounds have been widely studied in CO_2 capture. The representative absorbents are monoethanolamine (MEA)[18], diethanolamine

(DEA)[19], and methyldiethanolamine (MDEA)[20]. However, these amines still have certain limitations. For example, MEA and DEA are primary and secondary amines with limited CO_2 loadings, respectively. In addition, a high level of energy is required for amine regeneration due to the high stability of the carbamate produced by chemical absorptions. Although the tertiary amine MDEA has a large CO_2 loading and a low regeneration energy, its chemical absorption rate is slow[21]. In order to address the shortcomings of current organic amines and explore amines with good performance in CO_2 loading, regeneration energy, and chemical absorption rate, numerous researchers have studied the influence of organic amine structures on their performances through experiments and modeling methods. For example, Liu et al.[22] investigate the steric hindrance effect on the reaction rate constants of chemical reactions between CO_2 and amines that include MEA and its four different substituent products. Singh et al.[23] study the effects of chain length, side chain, number of functional groups (amine groups) and other factors on CO_2 absorption rates.

Although a number of experiments have been conducted in order to investigate the absorption properties of organic amines with different structures extensively in the last few decades, yet a significant number of potential high-performance molecules remain undiscovered. Compared with the experimental approach, the first principle-based molecular simulation methods (e.g., Density Functional Theory (DFT), Hartree-Fock, etc.) provide a relatively cost-effective means for screening or designing molecules with desired properties. DFT has been widely used to study the reaction kinetics of CO_2 absorption by organic amines[24]. For example, Silva et al.[25] employ the DFT

method to study the chemical reactions between CO_2 and amine systems, and analyze the important factors affecting the overall reactivity. Xie et al.[26] use the DFT method to calculate activation energies for the reactions between a series of substituted monoethanolamines and CO_2, and investigate the effect of substituents on reaction kinetics. On the basis of the experimental work of Chowhury[27], Rozanska et al.[28] study the absorption properties of 24 types of tertiary amine aqueous solutions through the DFT method and the molecular dynamics simulation, establishing a quantitatively accurate model for predictions of absorption rate constants. Nevertheless, their model has not considered primary/secondary amines and other non-aqueous solvents, which hinders the application of their model to explore more potential amines. Although the DFT method has been widely used by scholars to study the reactions between organic amines and CO_2, there is still no universal reaction kinetic mechanism model that is highly accurate and widely applicable. One of the largest challenges is that the conformational effect of transition states and reactants has a significant effect on reaction kinetics, but few efficient and automatic conformer search methods are available for transition states.

To this end, an efficient and automatic reactive site-based conformer search method for transition states is developed in this work. It is used to develop a universal reaction kinetic mechanism model based on the transition state theory and the DFT method for accurate predictions of CO_2 chemical absorption rate constants in various amine-solvent solutions involving primary, secondary, tertiary amines and water, methanol, ethanol solvents. By utilizing the transition state conformer search method,

the prediction accuracy of the reaction kinetic model is significantly enhanced. This paper is organized as follows. In the second section, the developments of the reaction kinetic model and the conformer search method for transition states are introduced. In the third section, the prediction results of the reaction kinetic model with/without the conformer search method are presented and discussed. Also, the influence mechanism of the transition state conformers on reaction kinetics of amine-based CO_2 chemical absorptions are studied by the analysis methods of weak interactions and reactive site charges.

2 Reaction kinetic model for amine-based carbon capture considering transition state conformers

In this section, a universal reaction kinetic model is developed for amine-based carbon capture, where a reactive site-based transition state conformer search method is proposed to enhance the model prediction accuracy. An overview of the development procedure of the reaction kinetic model and the relationship between the kinetic model and the transition state conformer search method is presented in **Fig. 1**.

In the first step (**Fig. 1(a)**), the rate-determining reaction steps of amine-based CO_2 chemical absorptions are first identified based on the reaction mechanisms. Then, in the second step (**Fig. 1(b)**), a reaction kinetic model is formulated by correlating chemical absorption rate constants (i.e., reaction rate constant in amine-solvent solutions k^{L}) with activation Gibbs free energies at liquid state based on the transition state theory and the hybrid solvation model. The model parameters are fitted with the DFT calculated activation energies and the experimental k^{L} through the least square method. With the

model parameters, k^{L} is able to be successfully predicted once the information of amine-solvent solutions is input to the reaction kinetic model. In the third step (**Fig. 1(c)**), a reactive site-based conformer search method for transition states is developed to further improve the prediction accuracy of the reaction kinetic model. The developed reaction kinetic model in this work involves all chemical absorption mechanisms for primary, secondary, and tertiary amines, as well as includes both aqueous and non-aqueous solvents. In the following subsections, the reaction kinetic mechanisms for amine absorptions, the transition state theory and hybrid solvation model used in the reaction kinetic model, as well as the conformer search method for transition states are presented in detail.

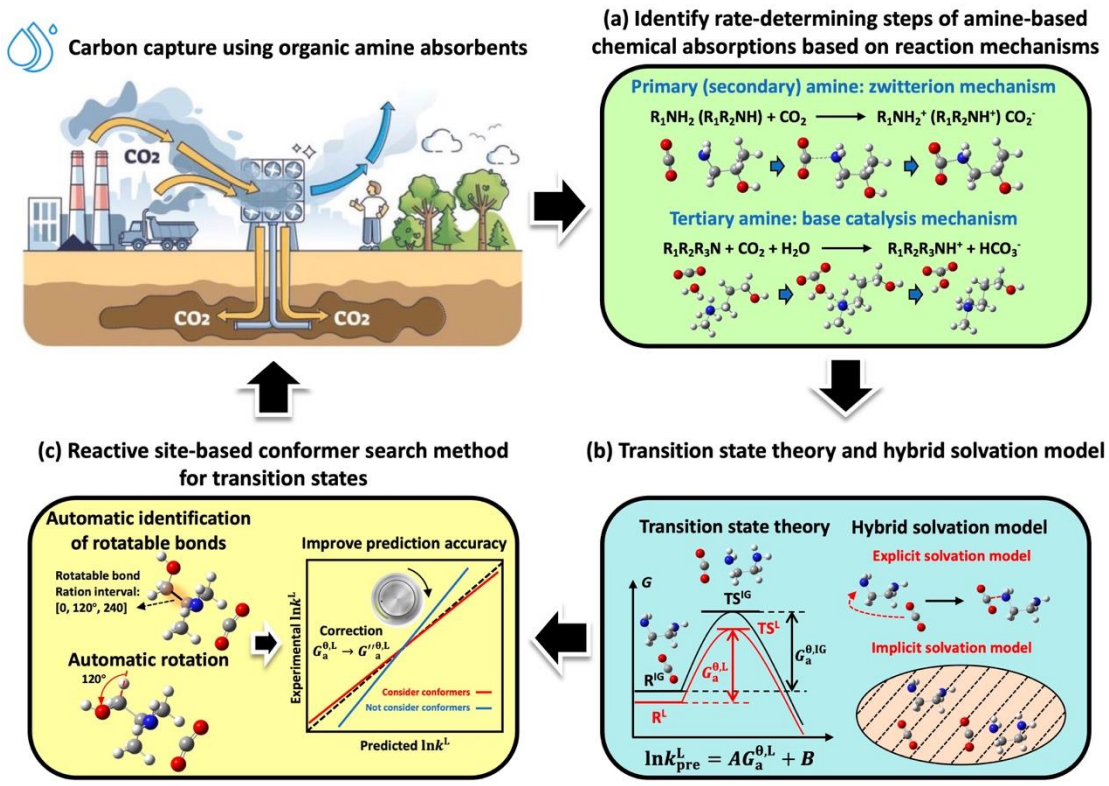

Fig. 1 An overview of the development procedure of the universal reaction kinetic model for amine-based carbon capture and the relationship between the kinetic model

and the reactive site-based transition state conformer search method.

2.1 Identify rate-determining steps of amine-based chemical absorptions based on reaction mechanisms

Amine refers to the product in which one or more hydrogen atoms in the ammonia molecule are replaced by hydrocarbon groups. According to the number of hydrogen atoms replaced in the amine molecule, amines can be divided into primary, secondary, and tertiary amines. The reaction mechanisms of amine-based CO_2 absorptions can be divided into three categories according to literatures.

The first category is the zwitterionic mechanism for primary and secondary amines[29], which includes two steps: the first step is the formation of an intermediate zwitterion (**Eq. (1)**), and the second step is the deprotonation of the zwitterion by reacting with a base (**Eq. (2)**). In these steps, R_1R_2NH represents a primary amine or a secondary amine if R_2 is a hydrogen atom or R_1 and R_2 are neither hydrogen atoms, respectively. The symbol B represents an amine, water, hydroxide or other substances that is used as a base.

$$R_1R_2NH + CO_2 \leftrightarrow R_1R_2NH^+CO_2^- \quad (1)$$

$$R_1R_2NH^+CO_2^- + B \leftrightarrow R_1R_2NCO_2^- + BH^+ \quad (2)$$

The second category is the trimolecular reaction mechanism for primary and secondary amines[30]. In this mechanism, the reaction between an amine and CO_2 forms an unstable complex rather than a zwitterion, and the complex is then regenerated into a carbamate through the direct reaction among an amine, CO_2, and a base molecule

(**Eq. (3)**).

$$R_1R_2NH + CO_2 + B \leftrightarrow CO_2 + R_1R_2NH \cdots B \leftrightarrow R_1R_2NCO_2^- + BH^+ \quad (3)$$

The third category is the base catalysis mechanism for tertiary amines[31], believing that the tertiary amine does not react directly with CO_2 like the primary and secondary amines as there is no H atom on the N atom in the tertiary amine. The mechanism holds the opinion that tertiary amines will form hydrogen bonds with water to increase the reactivity of CO_2 and water (**Eq. (4)**).

$$R_1R_2R_3N + CO_2 + H_2O \leftrightarrow R_1R_2R_3NH^+ + HCO_3^- \quad (4)$$

According to literatures[32, 33], researchers have compared the reaction energy barriers of two mechanisms (**Eq. (1)** and **Eq. (3)**) for primary and secondary amines through the DFT methods. The results show that the reaction energy barriers of the zwitterion mechanism (**Eq. (1)**) are lower than those of the trimolecular reaction mechanism (**Eq. (3)**), indicating that the zwitterionic mechanism is more suitable to describe the CO_2 chemical absorptions in primary and secondary amines. Besides, the literatures find that the rate of the second reaction step in the zwitterion mechanism is generally faster than that of the first step. Thus, the first reaction step in the zwitterionic mechanism is usually the rate-determining step. Therefore, this work employs the first step of the zwitterion mechanism (**Eq. (1)**) as the rate-determining reaction step to study the CO_2 chemical absorptions in primary and secondary amines. As for tertiary amines, the rate-determining reaction step (**Eq. (1)**) in the base catalysis mechanism is considered.

2.2 Transition state theory and hybrid solvation model

Based on the analyses of the amine-based chemical absorption mechanisms, the next step is to develop a universal reaction kinetic model for predictions of CO_2 chemical absorption rate constants. The kinetic model can be primarily formulated by the transition state theory, as shown in **Eqs. (5-6)**.

$$k^{\theta,\mathrm{L}} = \kappa \frac{k_\mathrm{B} T}{h} \prod_i \left(c_i^{\theta,\mathrm{L}}\right)^{\nu_i} \exp\left(-\frac{G_\mathrm{a}^{\theta,\mathrm{L}}}{RT}\right), i = \mathrm{TS}, \mathrm{R} \tag{5}$$

$$G_\mathrm{a}^{\theta,\mathrm{L}} = \sum_i \nu_i G_i^{\theta,\mathrm{L}} = \sum_i \nu_i \left(G_i^{\theta,\mathrm{IG}} + \Delta G_i^{\theta,\mathrm{p}\to\mathrm{c}} + \Delta G_i^{\theta,\mathrm{solv}}\right), i = \mathrm{TS}, \mathrm{R} \tag{6}$$

where $k^{\theta,\mathrm{L}}$ is the standard reaction rate constant in liquid phase, κ is the dimensionless transmission coefficient (assume to be a constant in this work), k_B is the Boltzmann constant, T is the reaction temperature, h is the Planck constant, $c_i^{\theta,\mathrm{L}}$ is the liquid phase standard state concentration of compound *i* ($c_i^{\theta,\mathrm{L}} = 1\ \mathrm{mol/L}$), ν_i is the stoichiometric coefficient of compound *i*, $G_\mathrm{a}^{\theta,\mathrm{L}}$ is the standard activation Gibbs free energy in liquid phase, R is the universal gas constant, TS represents the transition state, R represents the reactants. $G_i^{\theta,\mathrm{IG}}$ denotes the standard Gibbs free energies of compound *i* in gas phase, which is predicted by the DFT method. $\Delta G_i^{\theta,\mathrm{p}\to\mathrm{c}}$ is the Gibbs free energy change of compound *i* from a pressure-based standard state at 1 atm to a concentration-based standard state at 1 mol/L for an ideal gas ($\Delta G_i^{\theta,\mathrm{p}\to\mathrm{c}} = 7.91\ \mathrm{kJ/mol}$ at 298.15 K and 1 atm). $\Delta G_i^{\theta,\mathrm{solv}}$ is the standard solvation free energy of compound *i*.

Then, two adjustable parameters (C_1 and C_2) are added to **Eq. (5)** to correct the reaction kinetic model by minimizing the prediction errors between the predicted k^L ($k_\mathrm{pre}^\mathrm{L}$) and the experimental k^L ($k_\mathrm{exp}^\mathrm{L}$), as shown in **Eq. (7)**. Once the temperature and

pressure are determined, **Eq. (7)** can be converted to **Eq. (8)**.

$$k_{\mathrm{pre}}^{\mathrm{L}} = C_1 \kappa \frac{k_{\mathrm{B}} T}{h} \prod_i \left(c_i^{\theta,\mathrm{L}}\right)^{\nu_i} \exp\left(-\frac{C_2 G_{\mathrm{a}}^{\theta,\mathrm{L}}}{RT}\right), i = \mathrm{TS}, \mathrm{R} \tag{7}$$

$$\begin{aligned} \ln k_{\mathrm{pre}}^{\mathrm{L}} &= A G_{\mathrm{a}}^{\theta,\mathrm{L}} + B = A \sum_i \nu_i G_i^{\theta,\mathrm{L}} + B \\ &= A \sum_i \nu_i \left(G_i^{\theta,\mathrm{IG}} + \Delta G_i^{\theta,\mathrm{p}\to\mathrm{c}} + \Delta G_i^{\theta,\mathrm{solv}}\right) + B, i = \mathrm{TS}, \mathrm{R} \end{aligned} \tag{8}$$

where the new adjustable parameter A equals to $-C_2/RT$, and another new parameter B equals to $\ln\left(C_1 \kappa k_{\mathrm{B}} T \prod_i \left(c_i^{\theta,\mathrm{L}}\right)^{\nu_i} / h\right)$. These two parameters are fitted with the $k_{\mathrm{exp}}^{\mathrm{L}}$ and the DFT calculated $G_{\mathrm{a}}^{\theta,\mathrm{L}}$ through the least square method. Therefore, $G_i^{\theta,\mathrm{IG}}$ and $\Delta G_i^{\theta,\mathrm{solv}}$ are two key physical quantities that need to be calculated by the DFT method.

Considering that amine-solvent solutions play the roles of reactants and reaction solvents in chemical absorption systems, it is necessary to employ the hybrid solvation model to describe transition states in solvent environments. The hybrid solvation model is composed of the explicit and implicit solvation models. The explicit solvation model is carried out to determine the three-dimensional spatial relationship among amine, solvent and CO_2 by searching the transition states of rate-determining reactions. The implicit solvation model is used to simulate solvent environments during the transition state search process. The tasks of the transition state search and the frequency analysis for transition states are performed to obtain the thermal correction to standard Gibbs free energy $G_{\mathrm{TS}}^{\theta,\mathrm{corr}}$ through the DFT calculations with the method of B3LYP functional, the basis set of 6-31G(d), the dispersion correction based on the Becke-Johnson (BJ) damping function, and the implicit solvation model (Solvation Model based on Density (SMD)[34]) in Gaussian 09 software[35]. Afterwards, the task of

single point energy calculation is performed for the transition state to obtain total electronic energy E_{TS} with the method of M062x functional, the basis set of def2tzvp, the dispersion correction based on the zero damping function. $G_{TS}^{\theta,IG}$ is then calculated through $G_{TS}^{\theta,IG} = G_{TS}^{\theta,corr} + E_{TS}$. Next, the SMD model is carried out to obtain $\Delta G_{TS}^{\theta,solv}$, where the method of M052x functional and the basis set of 6-31G(d) are adopted in this step. Similar DFT tasks are performed for the reactants of amine, solvent, and CO_2 using the same DFT level.

2.3 Reactive site-based conformer search method for transition states

A molecule may have different conformational isomers with distinct Gibbs free energies due to the hydrogen-bonding effect, conjugation effect, and so on. Since a large number of N-H and O-H bonds in amine-solvent-CO_2 systems will form intermolecular hydrogen bonds and affect the reaction energy barriers[36], it is necessary to consider the influences of conformational effects of reactants and transition states on $G_a^{\theta,L}$.

The automatic conformer search method for reactants is available in known software, including Open Babel[37], Molclus[38], and so on. However, to our best knowledge, the known conformer search methods are hard to be directly applied to transition states as they are either generally worked to identify the minimum points rather than the saddle points along the potential energy surface[37] or need to set rotatable bonds manually[38]. Therefore, it is desirable to develop an efficient and automatic conformer search method for transition states to find the most stable transition state with the lowest energy among its conformers for each rate-determining reaction. To this end, an efficient and automatic reactive site-based conformer search

method for transition states is developed in this work. Its working principle is to freeze the reactive sites of transition states first, and then rotate the side chains that link to the reactive sites to find potential conformational isomers for transition states.

More specifically, the transition state conformer search method is carried out through three steps, as shown in **Fig. 2**. In the first step (**Fig. 2(a)**), the "confab" module in the Open Babel[37] software is employed to automatically identify the rotatable bonds and the rotation intervals for transition states. In this work, two modifications are made to the obtained rotatable bonds to avoid the Cartesian coordinate variances of the reactive sites. First, if two atoms linked by a certain rotatable bond both belong to the reactive sites, this rotatable bond is deleted. Second, the atomic numbers of the atoms close to the reactive sites need to be written on the left side of the rotatable bond string. For example, in **Fig. 2(a)**, the rotatable bond string "9-8" is given by the Open Babel software and it needs to be modified to "8-9". This is because the side chain attached to the atom on the right side of the rotatable bond string is set to be rotated in the next step. In the second step (**Fig. 2(b)**), the "gentor" module in the Molclus software[38] is employed to automatically generate a large number of "pseudo" conformational isomers through rotating the rotatable bonds according to the rotation intervals ergodically. In the third step (**Fig. 2(c)**), the semi-empirical DFT method (e.g., PM7) in the MOPAC software[39] is used to optimize the generated "pseudo" conformational isomers. During this process, the reactive sites are frozen. The optimized results are then processed with the "isostat" module in the Molclus software[38] to cluster similar conformational isomers of transition states. The obtained conformational isomers are

finally ranked according to their standard enthalpies of formation and the Boltzmann distribution at a certain temperature. Note that the reliability of ranking conformers depends on the energy calculation methods to some extent. It is suggested to select a certain number of top ranked conformers rather than only the top ranked one for further rigorous evaluations if the energy calculation methods are not rigorous.

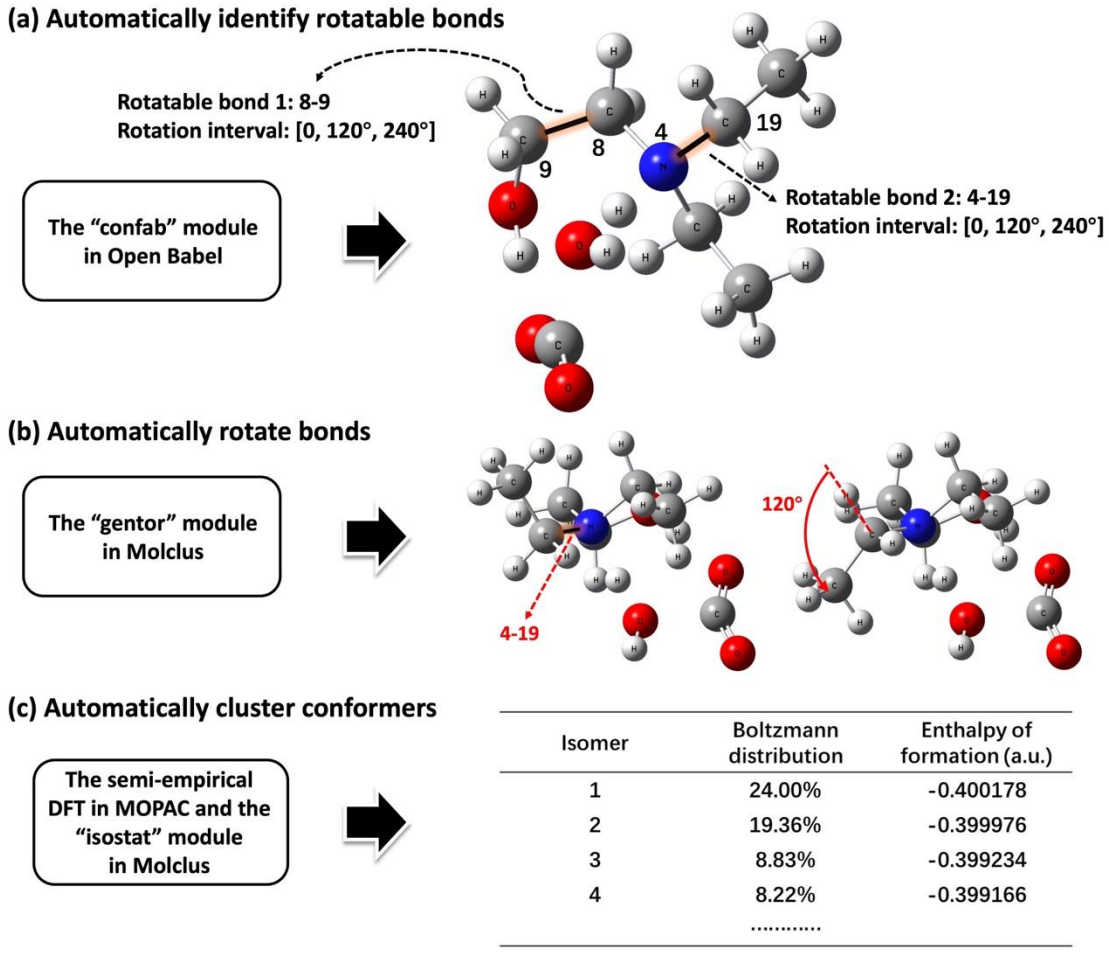

Fig. 2 The schematic diagram of the reactive site-based conformer search method for transition states.

After using the known conformer search method for reactants and the developed

reactive site-based conformer search method for transition states, a few top ranked conformers of reactants and transition states are respectively selected for further rigorous DFT calculations in this work. The corrected activation Gibbs free energies, $G'^{\theta,L}_{a}$ and $G''^{\theta,L}_{a}$, are calculated based on only the reactant conformer with the lowest $G^{\theta,L}_{R}$, as well as based on both the reactant and transition state conformers with the lowest $G^{\theta,L}_{R}$ and $G^{\theta,L}_{TS}$, respectively. Finally, the reaction kinetic model considering the conformational effect is developed by fitting the model parameters (*A* and *B* in **Eq. (8)**) with $G'^{\theta,L}_{a}(G''^{\theta,L}_{a})$ and k^{L}_{exp}. However, our conformer search approach has two shortcomings. One is that it fails to search the conformers of alicyclic rings. The other one is that it cannot handle on the molecule with too many rotatable bonds, as there will be a combinatorial explosion in sampling space. These shortcomings will be addressed by integrating our method with the simulated annealing approach based on molecular dynamics in the future work.

3 Results and discussions

3.1 Performance of reaction kinetic model for amine-based carbon capture

In this work, a total number of 21 different amine-solvent solutions with corresponding k^{L}_{exp} are used to develop a universal reaction kinetic model for predictions of amine-based CO_2 absorption rate constants, as shown in **Fig. 3**. Ten top ranked reactants and transition states obtained by the known conformer search method for reactants and the developed reactive site-based conformer search method for transition states are selected for each reaction system. The $G^{\theta,L}_{a}$, $G'^{\theta,L}_{a}$, and $G''^{\theta,L}_{a}$ of each reaction system are calculated through the DFT method without the consideration

of conformational effects, with the consideration of conformational effects for only reactants, and with the consideration of conformational effects for both reactants and transition states, respectively. The obtained $G_{\mathrm{a}}^{\theta,\mathrm{L}}/G'_{\mathrm{a}}{}^{\theta,\mathrm{L}}/G''_{\mathrm{a}}{}^{\theta,\mathrm{L}}$ are linearly fitted with $k_{\mathrm{exp}}^{\mathrm{L}}$ through **Eq. (8)**. Note that the reaction temperatures for all reaction systems are 298.15 K. **Fig. 4** shows the regression results of reaction kinetic models. **Tab. 1** gives the specific values of $G_{\mathrm{a}}^{\theta,\mathrm{L}}$, $G'_{\mathrm{a}}{}^{\theta,\mathrm{L}}$, $G''_{\mathrm{a}}{}^{\theta,\mathrm{L}}$ and $\ln k_{\mathrm{exp}}^{\mathrm{L}}$ for each reaction system. As shown in **Fig. 4**, the data points of primary/secondary amine-based reaction systems are basically distributed on the left side, while the data points of tertiary amine-based reaction systems are distributed on the right side. If the conformational effect is not considered for reactants and transition states (**Fig. 4(a)**), the distribution of each data point is relatively scattered, and the determination coefficient (R^2) of the model regression results is 0.764. If the conformer search methods are used for only reactants and both reactants and transition states, the R^2 of the reaction kinetic model has significantly improved from 0.764 to 0.819 and 0.764 to 0.943, respectively, indicating the necessity of considering the conformational isomer issue in developing reaction kinetic models and demonstrating the feasibility and effectiveness of our transition state conformer search method in further enhancing the prediction accuracy of the reaction kinetic model. The results are consistent with the fact that the closer the transition states and reactants are to their reality states (i.e., the lowest energy state), the more accurate the reaction kinetic model behaves.

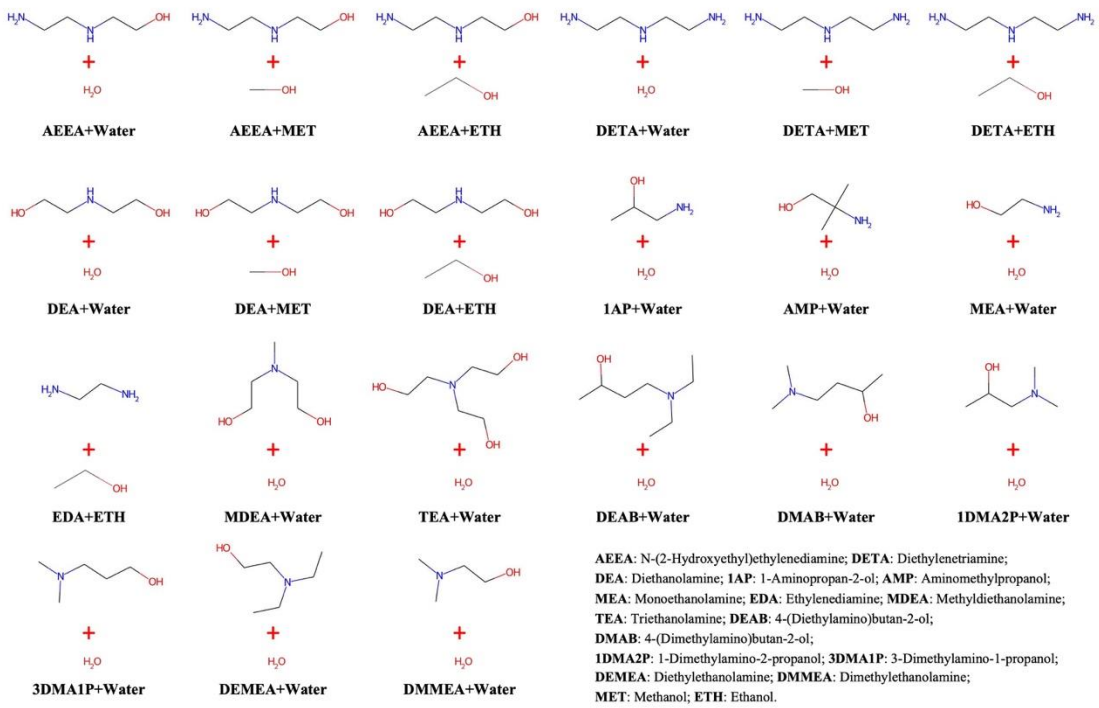

Fig. 3 The amine-solvent solutions studied in this work.

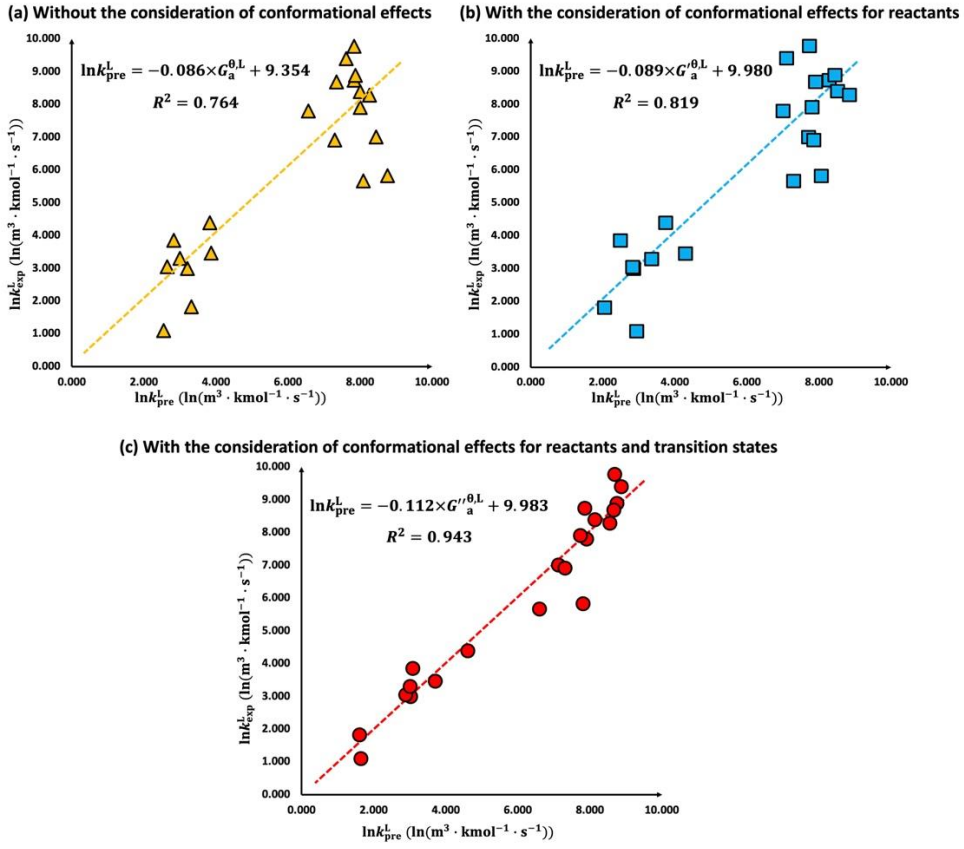

Fig. 4 The regression results of the reaction kinetic models.

https://doi.org/10.26434/chemrxiv-2023-8blq5 **ORCID:** https://orcid.org/0000-0002-3879-1827

Tab. 1 The values of DFT calculated activation Gibbs free energies and experimental reaction rate constants for each amine-solvent solution.

Amine-solvent solution	$G_a^{\theta,L}$ (kJ/mol)[a]	$G'^{\theta,L}_a$ (kJ/mol)[b]	$G''^{\theta,L}_a$ (kJ/mol)[c]	$\ln k_{exp}^{L}$ ($\ln(m^3 \cdot kmol^{-1} \cdot s^{-1})$)
AEEA-H_2O	20.318	32.412	9.992	9.401[40]
AEEA-MET	32.419	33.430	18.517	7.800[41]
AEEA-ETH	15.746	24.362	20.124	7.908[41]
DETA-H_2O	17.775	25.216	11.540	9.770[42]
DETA-MET	17.656	19.037	19.037	8.734[41]
DETA-ETH	17.236	17.236	11.083	8.892[41]
DEA-H_2O	10.620	25.512	25.512	7.003[43]
DEA-MET	6.931	21.526	19.427	5.823[19]
DEA-ETH	14.787	30.219	30.219	5.670[43]
1AP-H_2O	15.745	16.473	16.473	8.396[44]
AMP-H_2O	23.889	23.889	23.889	6.914[45]
MEA-H_2O	23.342	23.344	11.766	8.690[46]
EDA-ETH	12.791	12.791	12.791	8.284[41]
MDEA-H_2O	70.235	89.135	74.804	1.819[47]
TEA-H_2O	79.193	79.193	74.500	1.099[48]
DEAB-H_2O	75.834	84.177	61.600	3.855[49]
DMAB-H_2O	71.544	80.075	62.203	2.993[49]

1DMA2P-H_2O	77.972	80.423	63.319	3.044[48]
3DMA1P-H_2O	63.885	63.886	56.086	3.466[48]
DEMEA-H_2O	64.223	70.097	47.950	4.394[48]
DMMEA-H_2O	73.948	74.481	62.300	3.296[50]

3.2 Influence mechanism of transition state conformational isomers on activation Gibbs free energies

In this subsection, two analysis methods involving weak interactions and reactive site charges are carried out for the transition state conformers to provide insights into the influence mechanism of transition state conformers on activation Gibbs free energies. For the convenience of illustrating the energy differences between conformers in a reaction system, a baseline energy is set for one conformer at 0 kJ/mol, and the relative energies of the other two conformers are then calculated based on the baseline value. Here, the Independent Gradient Model based on Hirshfeld partition (IGMH)[51] method is utilized to make intuitive descriptions of the weak interactions. Besides, the Atomic Dipole moment Corrected Hirshfeld (ADCH)[52] method is used to determine the atomic charges of reactive sites in conformers, which is calculated using the Multiwfn[53] software and visualized by the VMD[54] software.

DETA-H_2O (secondary amine), a widely used amine-solvent solution, is first taken as an example, along with its three typical conformers of transition states (**Fig. 5**). The IGMH results for the transition state conformers in the DETA-H_2O system is shown in **Fig. 6**. The ADCH charge differences between the reactive sites of the C atom in CO_2

and the N atom in amine (1C-7N), as well as the relative activation Gibbs free energies of the transition state conformers in the DETA-H_2O system, are given in **Tab. 2**. From **Figs. 5** and **6**, it is seen that the O atom in CO_2 has a weak interaction (hydrogen-bonding interaction) with the H atom in amine among three conformers. This hydrogen-bonding interaction is beneficial to the attractions between 1C-7N reactive sites, the interaction of which is also identified in **Fig. 6**. From **Tab. 2** it is found that the ADCH charge difference of 1C-7N in the conformer (**Fig. 5(b)**) is larger than those of the other two conformers (**Figs. 5(a)** and **5(c)**), indicating that the reactants of CO_2 and amine are easier to react with each other through the minimum energy path that involves the transition state conformer (**Fig. 5(b)**). This result is also consistent with the qualitative ranking of relative activation Gibbs free energies, which confirms the validity of the calculated results regarding activation Gibbs free energies to some extent. The ADCH charge differences among reactive sites could provide an explanation for the variations in energy caused by conformational changes.

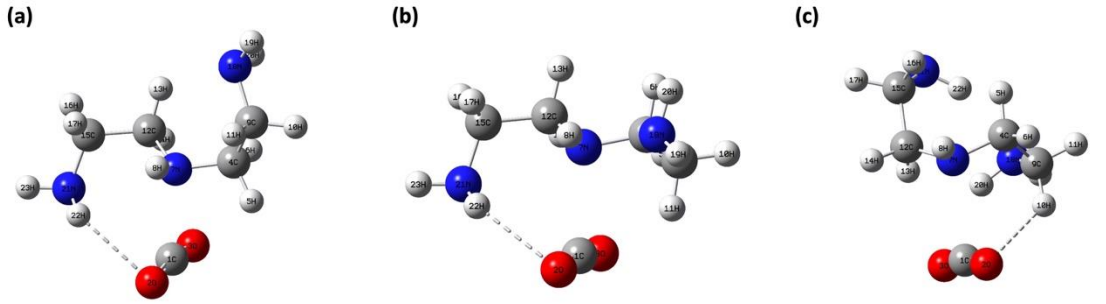

Fig. 5 Three typical conformers of transition states in the DETA-H_2O system.

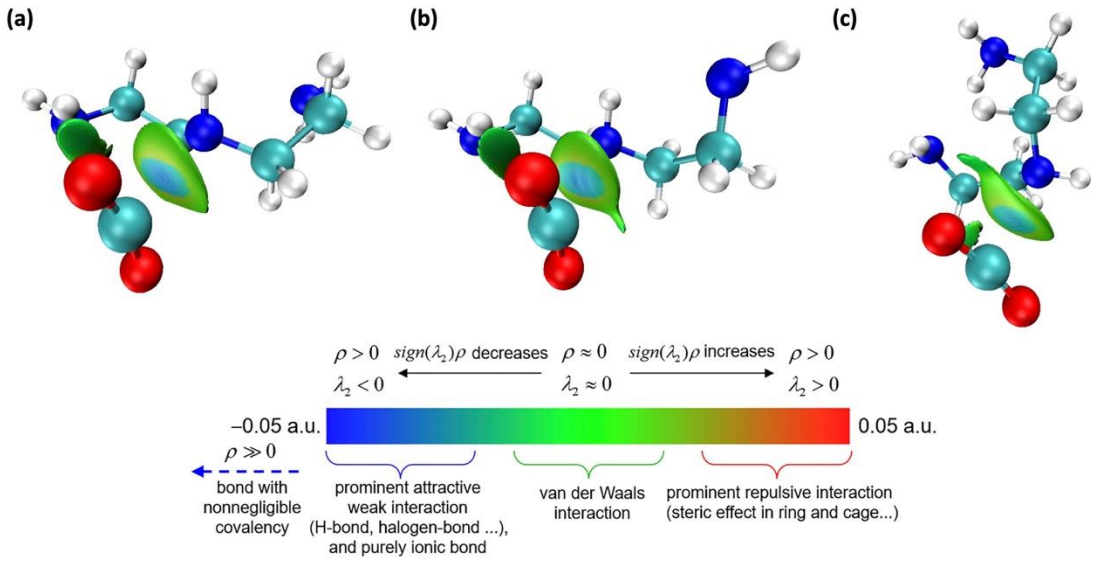

Fig. 6 The IGMH results for the transition state conformers in the DETA-H_2O system.

Tab. 2 The ADCH charge differences between the reactive sites of the C atom in CO_2 and the N atom in amine (1C-7N), as well as the relative activation Gibbs free energies of the transition state conformers in the DETA-H_2O system.

Conformer	ADCH charge difference of 1C-7N (a.u.)	$G''^{\theta,L}_{a}$ (kJ/mol)
(a)	0.4110	0
(b)	0.5437	-13.68
(c)	0.3896	8.59

MDEA-H_2O (tertiary amine), another commonly used amine-solvent solution, is also taken as an example, along with its three typical conformers of transition states (**Fig. 7**). The IGMH results for the transition state conformers in the MDEA-H_2O system is shown in **Fig. 8**. Note that there are two pairs of reactive sites in the MDEA-H_2O system as it follows the base catalysis mechanism of tertiary amines. Therefore,

the ADCH charge differences between the C atom in CO_2 and the O atom in water (1C-5O), those between the N atom in amine and the H atom in water (7N-4H), as well as the summation of the 1C-5O and 7N-4H charge differences are considered in this example. The ADCH charge differences, as well as the relative activation Gibbs free energies of the transition state conformers in the MDEA-H_2O system, are given in **Tab. 3**. As shown in **Fig. 7**, the O atom in CO_2 tends to form a hydrogen-bonding interaction with the H atom on the hydroxyl group in amine. Compared with the conformers (**Fig. 7(a)** and **7(b)**) that only have one hydrogen bond, there are two more hydrogen bonds in the conformer (**Fig. 7(c)**), including one interaction between the O atom in hydroxyl group and the H atom in water (8O-5H), and another interaction between the H atom in hydroxyl group and the O atom in CO_2 (14H-2O). **Fig. 8** also identifies the interactions observed in **Fig. 7** and the critical weak interactions among two pairs of reactive sites (1C-5O and 7N-4H). Although the number of hydrogen bonds in the conformer (**Fig. 7(c)**) is more than that in the conformers (**Fig. 7(a)** and **7(b)**) and the hydrogen-bonding interaction (8O-5H) is able to accelerate the reaction process by improving the 7N-4H attractions, the overall reaction process is still limited by the hydrogen-bonding interaction (14H-2O) according to the base catalysis mechanism of tertiary amines because the 14H-2O interaction cooperates with the hydrogen-bonding interaction (9H-3O) to hinder the attack of CO_2 to water. The above weak interaction analysis is able to explain why the activation Gibbs free energy of the conformer (**Fig. 7(c)**) is larger than those of the other two conformers (**Fig. 7(a)** and **7(b)**). From **Tab. 3** it is found that the summation of the ADCH charge differences of 7N-4H and 1C-5O in the conformer (**Fig.**

402 **7(b)**) is larger than those of the other two conformers (**Figs. 7(a)** and **7(c)**), indicating
403 that the reactants of CO_2 and amine are easier to react with each other through the
404 minimum energy path that involves the transition state conformer (**Fig. 7(b)**). This
405 result is also consistent with the qualitative ranking of relative activation Gibbs free
406 energies, which confirms the validity of the calculated results regarding activation
407 Gibbs free energies.

408 The analysis results of the DETA-H_2O and MDEA-H_2O systems highlight the
409 necessity of considering the impacts of the transition state conformer variations on
410 reactivities. The calculations of weak interactions and reactive site charges also
411 demonstrate the rationality of ranking for transition state conformers based upon
412 activation Gibbs free energies predicted by the conformer search method and DFT
413 calculations.

414

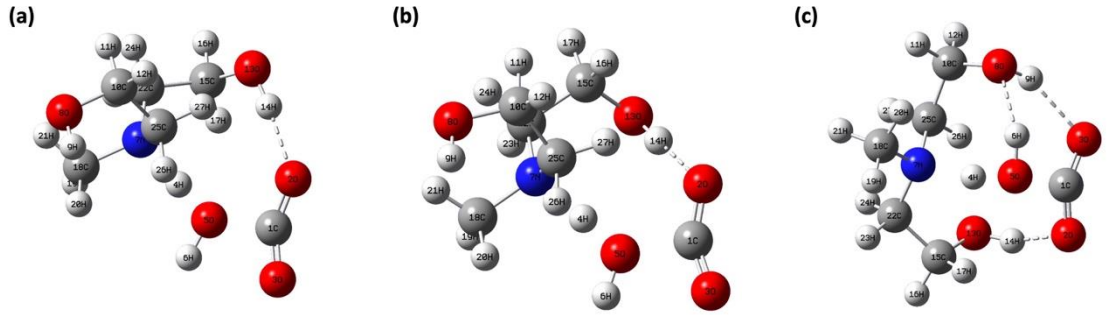

415

416 **Fig. 7** Three typical conformers of transition states in the MDEA-H_2O system.

417

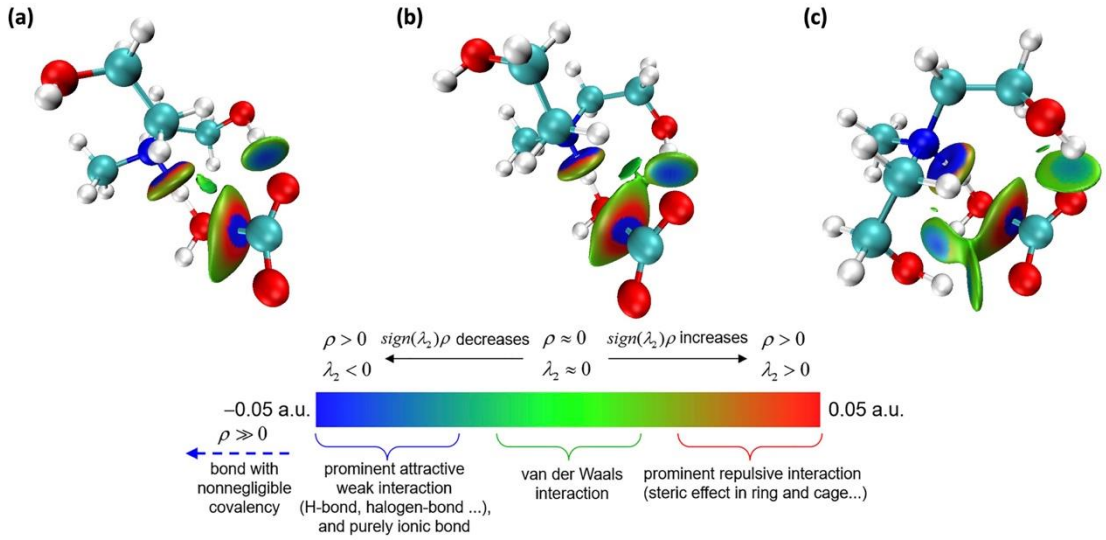

Fig. 8 The IGMH results for the transition state conformers in the MDEA-H_2O system.

Tab. 3 The ADCH charge differences between the reactive sites of the C atom in CO_2 and the O atom in water (1C-5O), and those of the N atom in amine and the H atom in water (7N-4H), as well as the relative activation Gibbs free energies of the transition state conformers in the MDEA-H_2O system.

Conformer	ADCH charge difference of 7N-4H (a.u.)	ADCH charge difference of 1C-5O (a.u.)	Total ADCH charge difference (a.u.)	$G''^{\theta,L}_{a}$ (kJ/mol)
(a)	0.1591	0.7662	0.9253	0
(b)	0.1640	0.7712	0.9352	-7.79
(c)	0.1711	0.7535	0.9246	9.54

3.3 Heuristic rules involving amine substituents

The variation of amine substituents often has a great impact on amine-based CO_2 absorption rate constants. For example, Jorgensen et al.[55] report that using the electron-donating amine substituents (e.g., NH_2CH_3, etc.) or increasing the number of substituents on amines is able to improve the interaction between CO_2 and amine. Xiao et al.[56] study ten commercial tertiary amines and find that the ethyl group and the side carbon chain are able to promote the activity of tertiary amine, and the increase of hydroxyl group is able to reduce the reaction rate. The study by Muchan et al.[57] shows that the increase in the number of amine groups is able to increase the absorption rate of CO_2. This work also finds that the $k_{\mathrm{exp}}^{\mathrm{L}}$ of three structurally similar amines (DETA, AEEA, and DEA) increase with the decrease of their numbers of hydroxyl groups and the increase of their numbers of amine groups, as shown in **Tab. 4**.

Here, some heuristic rules involving amine substituents are summarized as follows. These rules can be served as the structural constraints for the optimization-based mathematical programming model, which is able to design amines-based CO_2 absorbents in a high-throughput manner (e.g., DETA, AEEA, and DEA).

(1) The amine-based CO_2 absorption rates increase if the hydroxyl group in organic amines is replaced by the amine group. The amine group is an electron-donating group, which is able to enhance the electric charge density of the N atom in reactive sites of amines.

(2) The amine-based CO_2 absorption rates increase if the hydroxyl group is far away from the N atom in reactive sites of amines. Hydroxyl group is an electron-accepting group, which is capable of decreasing the electric charge density of the N

atom in reactive sites of amines (e.g., 3DMA1P and 1DMA2P).

Tab. 4 The relationship between the numbers of functional groups and the values of experimental reaction rate constants.

Amine-solvent system	Hydroxyl group	Amine group	$\ln k_{exp}^{L}$ ($\ln(m^3 \cdot kmol^{-1} \cdot s^{-1})$)
DETA-H_2O	0	2	9.770
AEEA-H_2O	1	1	9.401
DEA-H_2O	2	0	7.003

4 Conclusion

Reaction kinetics is a key evaluation criterion for amine-based carbon capture process. A universal reaction kinetic mechanism model is developed in this paper for predictions of reaction rate constants for CO_2 chemical absorptions based on the transition state theory, the DFT method, and the hybrid solvation model. The developed reaction kinetic model covers a wide range of 21 reaction systems involving primary/secondary/tertiary amines and aqueous/nonaqueous solvents. The key contribution of this work is proposing a reactive site-based conformational isomer search method for transition states. The proposed transition state conformer search method has significantly enhanced the prediction accuracy of the universal reaction kinetic model from R^2=0.819 to R^2=0.943, demonstrating its successful application in modeling the reaction kinetics of amine-based CO_2 chemical absorptions. Compared

with the semi-empirical and empirical modeling methods, our mechanism model only needs two adjustable parameters regressed by the experimental data, and has a strong interpretability for CO_2 absorption process. Two analysis methods of IGMH and ADCH involving weak interactions and reactive site charges, respectively, are also carried out to provide insights into the influence mechanism of transition state conformational isomers on activation Gibbs free energies. The analysis results verify the rationality of ranking transition state conformers by activation energies, confirming the effectiveness of our conformational isomer search method in searching for stable transition state conformers with high existing probability.

Despite the sound performance of our reaction kinetic model for predicting CO_2 absorption rate constants, other absorption properties, including absorption capacity, absorption solubility, desorption energy consumption, have not been considered in this paper. An optimization-based mathematical programming model consisting of the reaction kinetic model developed in this work, the property constraints of other absorption properties, and the heuristic rule-based structural constraints will be studied in our future research.

Acknowledge

The authors are grateful for the financial supports of NSFC (22208042, 22078041, 22278053), China Postdoctoral Science Foundation (2022M710578), and "the Fundamental Research Funds for the Central Universities" (DUT22YG218, DUT22LAB608).

Reference

1. IPCC, *Climate change 2022: mitigation of climate change*, in *Cambridge: Cambridge University Press*. 2022.
2. Metz, B., et al., *IPCC special report on carbon dioxide capture and storage*. 2005: Cambridge: Cambridge University Press.
3. Rubin, E.S., et al., *The outlook for improved carbon capture technology.* Progress in energy and combustion science, 2012. **38**(5): p. 630-671.
4. Feron, P., *Membranes for carbon dioxide recovery from power plants*, in *Carbon Dioxide Chemistry*. 1994, Elsevier. p. 236-249.
5. He, X.Z., *A review of material development in the field of carbon capture and the application of membrane-based processes in power plants and energy-intensive industries.* Energy Sustainability and Society, 2018. **8**.
6. Ishibashi, M., K. Otake, and S. Kanamori, *Study on CO_2 removal technology from flue gas of thermal power plant by physical adsorption method.* Greenhouse Gas Control Technologies, 1999: p. 95.
7. Builes, S., et al., *Microporous carbon adsorbents with high CO_2 capacities for industrial applications.* Physical Chemistry Chemical Physics, 2011. **13**(35): p. 16063-16070.
8. Rochelle, G.T., *Amine Scrubbing for CO_2 Capture.* Science, 2009. **325**(5948): p. 1652-1654.
9. Li, K., et al., *Systematic study of aqueous monoethanolamine (MEA)-based CO_2 capture process: Techno-economic assessment of the MEA process and its improvements.* Applied Energy, 2016. **165**: p. 648-659.
10. D'Alessandro, D.M., B. Smit, and J.R. Long, *Carbon dioxide capture: Prospects for new materials.* Angewandte Chemie International Edition, 2010. **49**(35): p. 6058-6082.
11. Yang, N., et al., *Aqueous ammonia (NH_3) based post combustion CO_2 capture: A review.* Oil & Gas Science and Technology-Revue D Ifp Energies Nouvelles, 2014. **69**(5): p. 931-945.
12. Ayittey, F.K., et al., *Parametric study and optimisation of hot K_2CO_3-based post-combustion CO_2 capture from a coal-fired power plant.* Greenhouse Gases-Science and Technology, 2020. **10**(3): p. 631-642.
13. Yang, Q.W., et al., *New insights into CO_2 absorption mechanisms with amino-acid ionic liquids.* Chemsuschem, 2016. **9**(8): p. 806-812.
14. Liu, S., et al., *Kinetics and new Bronsted correlations study of CO_2 absorption into primary and secondary alkanolamine with and without steric-hindrance.* Separation and Purification Technology, 2020. **233**.
15. Fang, M., et al., *Experimental study on CO_2 absorption into aqueous ammonia-based blended absorbents.* Energy Procedia, 2014. **61**: p. 2284-2288.
16. Qi, G., et al., *Integrated bench-scale parametric study on CO_2 capture using a carbonic anhydrase promoted K_2CO_3 solvent with low temperature vacuum stripping.* Industrial & Engineering Chemistry Research, 2016. **55**(48): p. 12452-12459.
17. Ramdin, M., T.W. de Loos, and T.J.H. Vlugt, *State-of-the-Art of CO2 Capture with Ionic Liquids.* Industrial & Engineering Chemistry Research, 2012. **51**(24): p. 8149-8177.
18. Sema, T., et al. *Mass transfer of CO_2 absorption in hybrid MEA-methanol solvents in packed column*. in *International Conference on Greenhouse Gas Technologies (GHGT)*. 2012. Kyoto, JAPAN.
19. Park, S.W., et al., *Reaction Kinetics of Carbon Dioxide with Diethanolamine in Polar Organic Solvents.* Separation Science and Technology, 2005. **40**(9): p. 1885-1898.

20. Ermatchkov, V., Á. Pérez-Salado Kamps, and G. Maurer, *Solubility of carbon dioxide in aqueous solutions of N-methyldiethanolamine in the low gas loading region.* Industrial & Engineering Chemistry Research, 2006. **45**(17): p. 6081-6091.
21. Liu, H.L., et al., *CO_2 absorption kinetics of 4-diethylamine-2-butanol solvent using stopped-flow technique.* Separation and Purification Technology, 2014. **136**: p. 81-87.
22. Liu, B., et al., *Reaction kinetics of the absorption of carbon dioxide (CO_2) in aqueous solutions of sterically hindered secondary alkanolamines using the stopped-flow technique.* Chemical Engineering Science, 2017. **170**: p. 16-25.
23. Singh, P. and G.F. Versteeg, *Structure and activity relationships for CO_2 regeneration from aqueous amine-based absorbents.* Process Safety and Environmental Protection, 2008. **86**(5): p. 347-359.
24. Yang, X., et al., *Computational modeling and simulation of CO_2 capture by aqueous amines.* Chemical Reviews, 2017. **117**(14): p. 9524-9593.
25. da Silva, E.F. and H.F. Svendsen, *Computational chemistry study of reactions, equilibrium and kinetics of chemical CO_2 absorption.* International Journal of Greenhouse Gas Control, 2007. **1**(2): p. 151-157.
26. Xie, H., et al., *Toward rational design of amines for CO_2 capture: Substituent effect on kinetic process for the reaction of monoethanolamine with CO_2.* Journal of Environmental Sciences, 2015. **37**: p. 75-82.
27. Chowdhury, F.A., et al., *CO_2 capture by tertiary amine absorbents: A performance comparison study.* Industrial & Engineering Chemistry Research, 2013. **52**(24): p. 8323-8331.
28. Rozanska, X., E. Wimmer, and F. de Meyer, *Quantitative Kinetic Model of CO2 Absorption in Aqueous Tertiary Amine Solvents.* Journal of Chemical Information and Modeling, 2021. **61**(4): p. 1814-1824.
29. Caplow, M., *Kinetics of carbamate formation and breakdown.* Journal of the American Chemical Society, 1968. **90**(24): p. 6795-6803.
30. Crooks, J.E. and J.P. Donnellan, *Kinetics and mechanism of the reaction between carbon-dioxide and amines in aqueous-solution.* Journal of the Chemical Society-Perkin Transactions 2, 1989(4): p. 331-333.
31. Donaldson, T.L. and Y.N. Nguyen, *Carbon dioxide reaction kinetics and transport in aqueous amine membranes.* Industrial & Engineering Chemistry Fundamentals, 1980. **19**(3): p. 260-266.
32. Yamada, H., et al., *Density functional theory study on carbon dioxide absorption into aqueous solutions of 2-amino-2-methyl-1-propanol using a continuum solvation model.* The Journal of Physical Chemistry A, 2011. **115**(14): p. 3079-3086.
33. Xie, H.B., et al., *Reaction mechanism of monoethanolamine with CO_2 in aqueous solution from molecular modeling.* Journal of Physical Chemistry A, 2010. **114**(43): p. 11844-11852.
34. Marenich, A.V., C.J. Cramer, and D.G. Truhlar, *Universal solvation model based on solute electron density and on a continuum model of the solvent defined by the bulk dielectric constant and atomic surface tensions.* The Journal of Physical Chemistry B, 2009. **113**(18): p. 6378-6396.
35. *Gaussian 09W Rev. D.01 [computer program].* Wallingford, CT: Gaussian, Inc., 2016.
36. Wang, K., X. Shan, and X. Chen, *Electron propagator theory study of 2-aminoethanol conformers.* Journal of Molecular Structure: THEOCHEM, 2009. **909**(1): p. 91-95.
37. O'Boyle, N.M., et al., *Open Babel: An open chemical toolbox.* Journal of Cheminformatics, 2011. **3**.
38. Lu, T., *Molclus program, Version 1.9.9.7.* http://www.keinsci.com/research/molclus.html, 2021.

39. Stewart, J.J.P., *MOPAC: A semiempirical molecular orbital program.* Journal of Computer-Aided Molecular Design, 1990. **4**(1): p. 1-103.
40. Ma'mun, S., V.Y. Dindore, and H.F. Svendsen, *Kinetics of the reaction of carbon dioxide with aqueous solutions of 2-((2-aminoethyl)amino)ethanol.* Industrial & Engineering Chemistry Research, 2007. **46**(2): p. 385-394.
41. Zhong, N., et al., *Reaction kinetics of carbon dioxide (CO_2) with diethylenetriamine and 1-amino-2-propanol in nonaqueous solvents using stopped-flow technique.* Industrial & Engineering Chemistry Research, 2016. **55**(27): p. 7307-7317.
42. Hartono, A., E.F. da Silva, and H.F. Svendsen, *Kinetics of carbon dioxide absorption in aqueous solution of diethylenetriamine (DETA).* Chemical Engineering Science, 2009. **64**(14): p. 3205-3213.
43. Sada, E., et al., *Chemical-kinetics of the reaction of carbon-dioxide with ethanolamines in nonaqueous solvents.* Aiche Journal, 1985. **31**(8): p. 1297-1303.
44. Henni, A., J. Li, and P. Tontiwachwuthikul, *Reaction kinetics of CO_2 in aqueous 1-amino-2-propanol, 3-amino-1-propanol, and dimethylmonoethanolamine solutions in the temperature range of 298−313k using the stopped-flow technique.* Industrial & Engineering Chemistry Research, 2008. **47**(7): p. 2213-2220.
45. Jamal, A., A. Meisen, and C. Jim Lim, *Kinetics of carbon dioxide absorption and desorption in aqueous alkanolamine solutions using a novel hemispherical contactor—II: Experimental results and parameter estimation.* Chemical Engineering Science, 2006. **61**(19): p. 6590-6603.
46. Versteeg, G.F., L.A.J. Van Dijck, and W.P.M. Van Swaaij, *On the kinetics between CO_2 and alkanolamines both in aqueous and non-aqueous solutions. An overview.* Chemical Engineering Communications, 1996. **144**(1): p. 113-158.
47. Rinker, E.B., S.A. Sami, and O.C. Sandall, *Kinetics and modelling of carbon dioxide absorption into aqueous solutions of N-methyldiethanolamine.* Chemical Engineering Science, 1995. **50**(5): p. 755-768.
48. Kadiwala, S., A.V. Rayer, and A. Henni, *Kinetics of carbon dioxide (CO_2) with ethylenediamine, 3-amino-1-propanol in methanol and ethanol, and with 1-dimethylamino-2-propanol and 3-dimethylamino-1-propanol in water using stopped-flow technique.* Chemical Engineering Journal, 2012. **179**: p. 262-271.
49. Singto, S., et al., *The effect of chemical structure of newly synthesized tertiary amines used for the post combustion capture process on carbon dioxide (CO_2): Kinetics of CO_2 absorption using the stopped-flow apparatus and regeneration, and heat input of CO_2 regeneration.* Energy Procedia, 2017. **114**: p. 852-859.
50. Versteeg, G.F. and W.P.M. van Swaaij, *On the kinetics between CO_2 and alkanolamines both in aqueous and non-aqueous solutions—II. Tertiary amines.* Chemical Engineering Science, 1988. **43**(3): p. 587-591.
51. Lu, T. and Q. Chen, *Independent gradient model based on Hirshfeld partition: A new method for visual study of interactions in chemical systems.* Journal of Computational Chemistry, 2022. **43**(8): p. 539-555.
52. Lu, T. and F. Chen, *Atomic dipole moment corrected hirshfeld population method.* Journal of Theoretical and Computational Chemistry, 2012. **11**(01): p. 163-183.
53. Lu, T. and F. Chen, *Multiwfn: a multifunctional wavefunction analyzer.* Journal of Computational Chemistry, 2012. **33**(5): p. 580-592.
54. Humphrey, W., A. Dalke, and K. Schulten, *VMD: Visual molecular dynamics.* Journal of Molecular

619 Graphics, 1996. **14**(1): p. 33-38.
620 55. Jorgensen, K.R., T.R. Cundari, and A.K. Wilson, *Interaction energies of CO_2-amine complexes:*
621 *Effects of amine substituents.* The Journal of Physical Chemistry A, 2012. **116**(42): p. 10403-10411.
622 56. Xiao, M., et al., *A study of structure–activity relationships of commercial tertiary amines for post-*
623 *combustion CO_2 capture.* Applied Energy, 2016. **184**: p. 219-229.
624 57. Muchan, P., et al., *Effect of number of amine groups in aqueous polyamine solution on carbon*
625 *dioxide (CO_2) capture activities.* Separation and Purification Technology, 2017. **184**: p. 128-134.
626